The importance of Fabry–Pérot resonance and the role of shielding in subwavelength imaging performance of multiwire endoscopes

Atiqur Rahman,[1] Pavel A. Belov,[1,a)] Mário G. Silveirinha,[2] Constantin R. Simovski,[3] Yang Hao,[1] and Clive Parini[1]
[1]*Department of Electronic Engineering, Queen Mary University of London, Mile End Road, London E1 4NS, United Kingdom*
[2]*Instituto de Telecomunicações, Universidade de Coimbra, 3030 Coimbra, Portugal*
[3]*Radio Lab., Helsinki University of Technology, P.O. Box 3000, FIN-02015 HUT, Finland*

(Received 24 October 2008; accepted 31 December 2008; published online 22 January 2009)

Multiwire endoscopes may enable the manipulation of the electromagnetic field in the subwavelength scale. Recently, two different configurations of such devices have been proposed. Here, we compare the imaging performance of the imaging device introduced by Belov *et al.* [Phys. Rev. B **73**, 033108 (2006)] and by Silveirinha *et al.* [Phys. Rev. B **75**, 035108 (2007)] with the shielded multiwire endoscope described by Shvets *et al.* [Phys. Rev. Lett. **99**, 053903 (2007)]. It is demonstrated that the performance of the latter may be strongly affected by the presence of a metallic shield around the endoscope and by poor matching between the endoscope and free space. Our results show that the metallic shield is completely unnecessary and emphasize the importance of tuning the length of the wires according to the Fabry–Pérot resonance condition, as proposed by Belov *et al.* [Phys. Rev. B **73**, 033108 (2006)]. © *2009 American Institute of Physics*.
[DOI: 10.1063/1.3073714]

Recent studies have shown that a bundle of parallel metallic wires may enable the transmission of the subwavelength details of an electromagnetic image to a distance larger than the wavelength.[1–4] Such manipulations of the electromagnetic field in the subwavelength spatial scale are based on the transformation of the whole spectrum of spatial harmonics generated by the source, including evanescent waves, into propagating eigenmodes of a metamaterial. This regime of operation is known as "canalization" and enables the propagation of the subwavelength fine details across a planar metamaterial slab, provided the thickness of the slab is tuned to obey the Fabry–Pérot (FP) resonance condition. The canalization regime was studied at the microwave,[1–3,5,6] infrared,[4,7,8] and even visible[9,10] domains. It has been used for realization of subwavelength imaging by photonic crystals and, in this context, it is also known as self-collimation,[11–13] directed diffraction,[14] and tunneling.[15] It is well established that an array of metallic wires can be operated in the canalization regime up to infrared frequencies due to the anomalous waveguiding properties of the quasi-transverse electromagnetic modes supported by the wires and that such effect is weakly dependent on losses and on the plasmonic properties of the metal.[4,7,8]

In a recent work, Shvets *et al.*[16] introduced a multiwire endoscope formed by an array of shielded metallic wires to image the near-field. Such setup differs in two essential points from the configuration considered in our previous works such that[1–4] (i) the bundle of wires is surrounded by a metallic shield and (ii) the length of the metallic wires is assumed to be irrelevant (i.e., the imaging properties are assumed to be independent of the length of the wires). Here, we compare the performances of the two imaging strategies and demonstrate with full wave simulations that the modifications considered in Ref. 16 do not lead to any improvement, but that on the contrary may dramatically affect the quality of the imaging.

To this end, we studied the imaging properties of a multiwire endoscope with exactly the same parameters as suggested in Ref. 16 using the full-wave electromagnetic simulator.[17] The endoscope is formed by an array of 25 $\times$25 metal wires (see Fig. 1); this corresponds to the number of wires suggested in Ref. 16 for a practical endoscope. As in Ref. 16, the length of the wires is taken equal to $4\lambda/3$ at the frequency of operation of 60 THz. As can be seen in Fig. 2, the imaging provided by such endoscope has very poor quality and the image at the output plane has hardly anything to do with the image at the source plane.

Our previous theoretical and experimental studies of multiwire systems[1–8] allow us to conclude that the endoscope does not operate properly because of two reasons. First, the endoscope is coated by a metal shield, when such a kind of shielding actually greatly reduces and limits the performance. Indeed, in subwavelength structures the electric field can be described to a good approximation by an electric po-

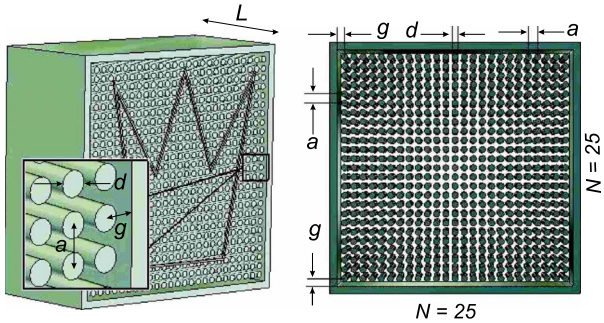

FIG. 1. (Color online) Geometry of the 25$\times$25 multiwire endoscope proposed in Ref. 16 for operation at $\lambda=5$ μm. The wires have length $L=4\lambda/3=6.67$ μm and diameter $d=\lambda/15=333$ nm. The period of the array is $a=\lambda/10=500$ nm and $g=d+\lambda/20=400$ nm. The near-field source is shaped in the form of a crown and is placed at the distance $0.07\lambda=350$ nm away from the endoscope.

a)Electronic mail: pavel.belov@elec.qmul.ac.uk.

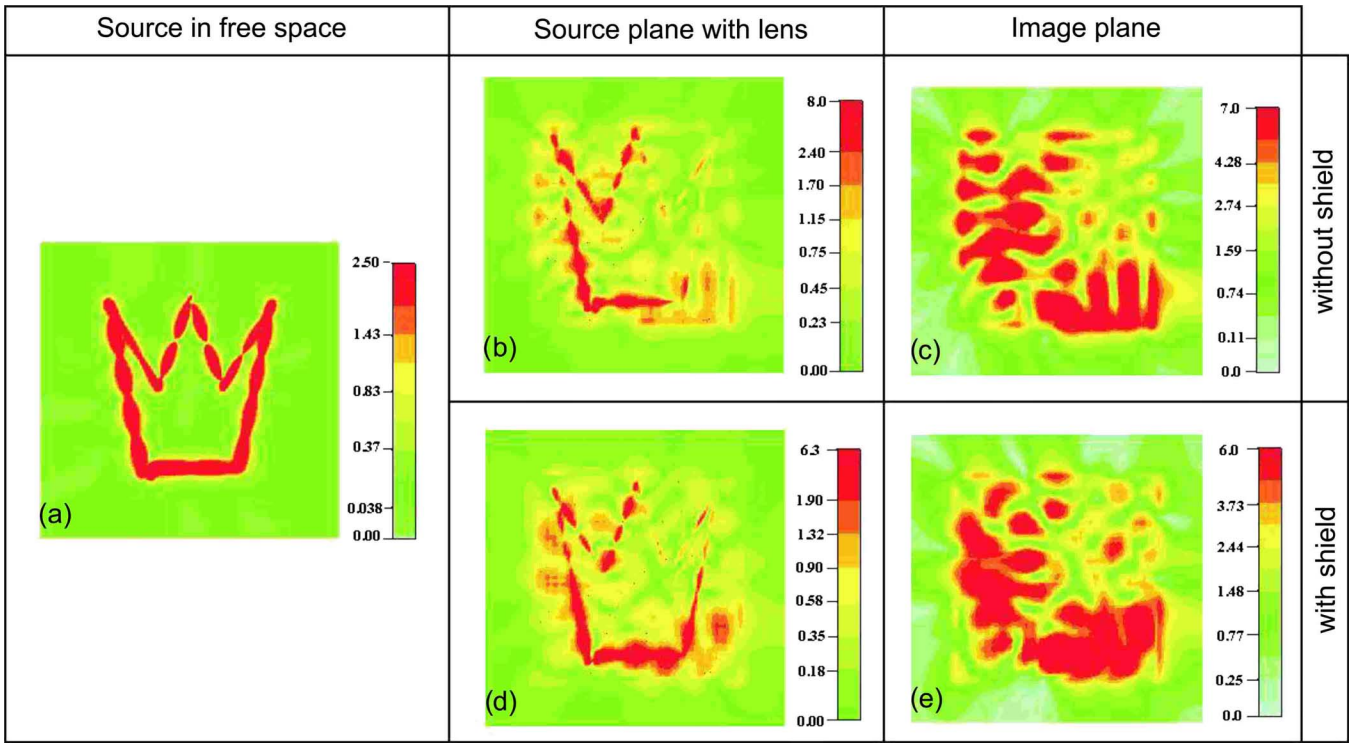

FIG. 2. (Color online) Numerical simulation at 60 THz ($\lambda=5$ μm). (a) Amplitude of the near field created by the source at the input interface of the endoscope when the interaction between the endoscope and the source is neglected. [(b) and (d)] Same as (a) but in the presence of the endoscope. The near-field is corrupted by reflections and by the excitation of guided modes. [(c) and (e)] Image at the output interface of the endoscope. The crown-shaped source is not discernible. The distributions (b) and (c), and (b) and (d), are for the endoscopes with and without shield, respectively.

tential. The multiwire system basically behaves as a "sampler" of electric potential. Such property implies that the period of the array roughly determines the resolution of the system. However, the presence of the metal shield forces the electric potential to be constant around a contour very close to the object to be imaged. This implies that the electric field distribution near the considered object is corrupted by the presence of the endoscope [see Figs. 2(d), 2(e), 4(d), and 4(e)]. In other words, diffraction by the metal shield may be extremely harmful to image formation. The second reason that explains the results of Fig. 2 is that an array of metallic wires can be used for sensing and guiding on the subwavelength scale only if the length of the wires is tuned to obey the FP resonance condition. This property was ignored in Ref. 16 whereas it is of fundamental importance in order that the fields can be effectively sensed by the endoscope. These problems can be avoided by using a multiwire endoscope with no metallic shield and thickness tuned to obey the FP resonance condition. In this case, as demonstrated in Ref. 18, because of the all-spatial-spectrum FP resonance, the multiwire endoscope does not produce any diffraction effects. The FP condition enhances the sensing properties, enables a nearly perfect transmission of the image, and guarantees the absence of strong reflections from the endoscope, which otherwise perturb the near field distribution of the source.

The importance of tuning the length of the endoscope to be an integer multiple of half wavelength can be better understood by the well-known input impedance expression of a transmission line (see Fig. 3),

$$Z_i = Z_0 \frac{Z_{\text{load}} + jZ_0 \tan(\beta L)}{Z_0 + jZ_{\text{load}} \tan(\beta L)}. \quad (1)$$

For any length $L=n\lambda/2$, the endoscope is effectively invisible and thus produces no reflection. In the case of a large deviation from $n\lambda/2$, the reflection effects may perturb the image formation at the source plane. Several theoretical and experimental studies[2,4] show that if the frequency of operation does not correspond to a FP resonance, the image may also be severely distorted (see Fig. 2) due to the excitation of guided modes supported by the wire medium slab and studied in detail in Ref. 6. This is a very general behavior characteristic of arrays of parallel wires and of tapered arrays, as shown in Ref. 19, where a threefold magnification was demonstrated using an array of 21×21 wires.

The thickness of the endoscope considered in Ref. 16 is $4\lambda/3$ at 60 THz, which deviates significantly from the FP resonance condition. As discussed above, this originates very strong reflections and the excitation of guided modes, which ultimately prevent the formation of a discernible image. When the source generating the crown-shaped near-field distribution [Fig. 2(a)] is placed next to the endoscope the near field becomes totally corrupted at the source plane [see Figs. 2(b) and 2(d)], independent of the presence or absence of the metallic shield [compare Figs. 2(b) and 2(d)]. Respectively, no identifiable image having the shape of a crown is observed as the fields get totally distorted by the guided modes [see Figs. 2(c) and 2(e)].

However, if the frequency of operation is increased to 66.2 THz, ensuring that the total thickness of the endoscope is equal to $3\lambda/2$ and that the FP resonance condition is veri-

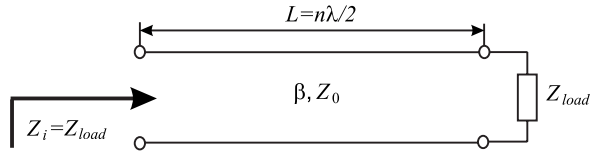

FIG. 3. Transmission line model of the endoscope.

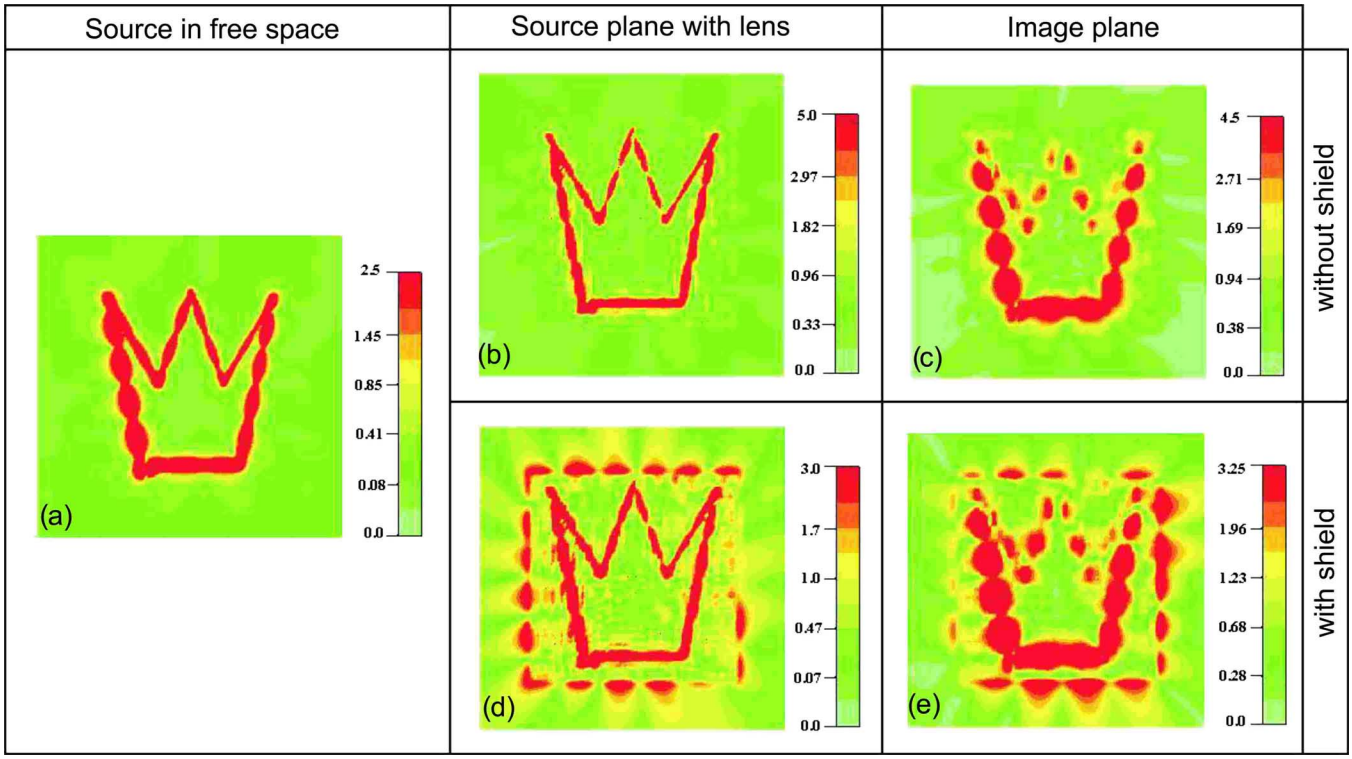

FIG. 4. (Color online) The same as Fig. 2, but at 66.2 THz, which corresponds to a FP resonance ($\lambda=4.53$ μm). The crown-shaped source is clearly reproduced at the output plane. Significant distortions around the boundary of the endoscope are observed when the metallic shield is present.

fied, the fields at the source plane [see Figs. 4(b) and 4(d)] may mimic very closely the fields created by the source in the free space [see Fig. 4(a)]. In contrast with the operation at 60 THz, no harmful reflected field is noticed in the source plane except for the case with metallic shield where some reflections can be traced [see Fig. 4(d)]. At the image plane, the crown-shaped field distribution is clearly visible, consistent with the fact that the FP condition improves the sensing ability and hence the fidelity of the system. Notice that the strong fields along a square boundary around the crown are caused by diffraction by the metal shield and that these are completely absent if the shield is removed.

In conclusion, it was shown that the multiwire endoscope proposed in Ref. 16 may not provide a satisfactory imaging performance. This happens because the thickness of the endoscope is not tuned to obey the FP resonance condition, which results in a mismatch between the device and the free space that causes strong reflections and the excitation of guided modes that totally distort the image. Moreover, the presence of the metallic shield around the array of wires leads to diffraction effects, which also prevent proper formation of the image. When the shield is removed and the FP resonance condition is verified, the endoscope becomes the multiwire system studied in Refs. 1–8, which exhibits an excellent subwavelength imaging performance.

P. A. Belov acknowledges financial support by EPSRC Advanced Research Fellowship EP/E053025/1.

[1] P. A. Belov, Y. Hao, and S. Sudhakaran, Phys. Rev. B **73**, 033108 (2006).
[2] P. A. Belov, Y. Zhao, S. Sudhakaran, A. Alomainy, and Y. Hao, Appl. Phys. Lett. **89**, 262109 (2006).
[3] P. A. Belov, Y. Zhao, S. Tse, P. Ikonen, M. G. Silveirinha, C. R. Simovski, S. Tretyakov, Y. Hao, and C. Parini, Phys. Rev. B **77**, 193108 (2008).
[4] M. Silveirinha, P. Belov, and C. Simovski, Phys. Rev. B **75**, 035108 (2007).
[5] P. A. Belov, C. R. Simovski, and P. Ikonen, Phys. Rev. B **71**, 193105 (2005).
[6] P. A. Belov and M. G. Silveirinha, Phys. Rev. E **73**, 056607 (2006).
[7] M. Silveirinha, Phys. Rev. E **73**, 046612 (2006).
[8] M. G. Silveirinha, P. A. Belov, and C. R. Simovski, Opt. Lett. **33**, 1726 (2008).
[9] P. Belov and Y. Hao, Phys. Rev. B **73**, 113110 (2006).
[10] X. Li, S. He, and Y. Jin, Phys. Rev. B **75**, 045103 (2007).
[11] J. Witzens, M. Loncar, and A. Scherer, IEEE J. Sel. Top. Quantum Electron. **8**, 1246 (2002).
[12] Z.-Y. Li and L.-L. Lin, Phys. Rev. B **68**, 245110 (2003).
[13] J. L. Garcia-Pomar and M. Nieto-Vesperinas, Opt. Express **13**, 7997 (2005).
[14] H.-T. Chien, H.-T. Tang, C.-H. Kuo, C.-C. Chen, and Z. Ye, Phys. Rev. B **70**, 113101 (2004).
[15] C.-H. Kuo and Z. Ye, Phys. Rev. E **70**, 056608 (2004).
[16] G. Shvets, S. Trendafilov, J. B. Pendry, and A. Sarychev, Phys. Rev. Lett. **99**, 053903 (2007).
[17] CST MICROWAVE STUDIO®, CST Computer Simulation Technology AG, www.cst.com.
[18] Y. Zhao, P. Belov, and Y. Hao, Opt. Express **14**, 5154 (2006).
[19] P. Ikonen, C. Simovski, S. Tretyakov, P. Belov, and Y. Hao, Appl. Phys. Lett. **91**, 104102 (2007).